JPEDAV (2016) 37:664–671
DOI: 10.1007/s11669-016-0493-8
1547-7037 ©ASM International

Investigation of the Mg-Rich Part of the Mg-Dy-Sm Phase Diagram

E.A. Lukyanova, L.L. Rokhlin, T.V. Dobatkina, I.G. Korolkova, and I.E. Tarytina

(Submitted May 10, 2016; in revised form July 28, 2016; published online August 25, 2016)

Constitution of the Mg-rich part of the ternary phase diagram of Mg with two rare-earth metals, Mg-Dy-Sm was experimentally investigated for the first time using optical and scanning electron microscopy (SEM) with electron probe microanalysis (EPMA), x-ray diffraction and differential thermal analysis. In equilibrium with Mg solid solution only two solid phases were found, each of them being the riches by Mg compound in the respective binary systems, $Mg_{24}Dy_5$ and $Mg_{41}Sm_5$. Each of these compounds can also dissolve some other rare-earth metal. There is significant combine solubility of Dy and Sm in Mg solid solution, which decreases with lowering temperature. In the studied part of the Mg-Dy-Sm system one invariant four-phase equilibrium of $L + (Mg_{24}Dy_5) \leftrightarrows (Mg) + (Mg_{41}Sm_5)$ exists, which takes place at 535 °C. A number of isothermal partial sections and one temperature-composition section of the Mg-Dy-Sm phase diagram were constructed.

Keywords magnesium alloys, phase equilibria, rare-earth metals, solid solutions, ternary phase diagrams

1. Introduction

Magnesium-based alloys are widely used in industry. They have the main advantage of quite favorable combination of the low density and sufficiently high strength properties. This fact makes the magnesium-based alloys very attractive light structural materials for the applications in aircraft, space, automotive, etc. industries, where low own weight of constructions is of a great importance.[1,2] Strength properties are principal parameters for structural material. The alloying of magnesium with rare-earth metals allows one as rule to obtain light magnesium-based alloys with the high strength, in particular, at elevated, up to 300 °C, temperatures.[3–8] However, the effect of individual rare-earth metals on magnesium may be quite different depending on the atomic number of the metals. Besides, their action can be changed, if two or more rare-earth metals together are added to magnesium.[9–12] The Mg-Dy-Sm compositions are supposed to be alloys, for which high strength properties can be expected. The specific feature of this system is the presence of two rare-earth metals of different subgroups. Dy belongs to the yttrium subgroup of the rare-earth metals and Sm belongs to the cerium subgroup. The ternary Mg-Dy-Sm system is of interest from the standpoint of the possible effect of each of the rare-earth metals on the behavior of the other in the alloys and their interaction should be revealed in the Mg-Dy-Sm phase diagram. We know no data on investigations of the Mg-Dy-Sm phase diagram. Thus, the aim of this work was to study equilibria in the system. The favorable effect of the rare-earth metals on the strength properties of magnesium usually takes place at the rare-earth concentrations corresponding to the magnesium-based solid solution and slightly higher. Therefore, in this study, we consider only Mg-rich part of the Mg-Dy-Sm phase diagram.

1.1 Adjoining Binary Systems

The both adjoining binary Mg-Dy and Mg-Sm phase diagrams were studied in the whole concentration ranges.[13] The Mg-rich parts of both Mg-Dy and Mg-Sm phase diagrams are of the eutectic type with the certain solubility of the rare-earth metals in solid Mg, which decreases with decreasing temperature. According to data of,[14] in which the Mg-rich alloys of the Mg-Dy system were studied in detail, the eutectic point corresponds to 46 mass% Dy and 561 °C. According to recent data,[15] the eutectic of the Mg-Sm system corresponds to 35 mass% Sm and 530 °C. The both systems significantly differ in rare-earth metal solubility in solid magnesium. The maximal Dy solubility in solid Mg at the eutectic temperature is 25.8 mass%[14]; the Sm solubility is 5.8 mass%.[16] The $Mg_{24}Dy_5$ (Pearson symbol *cI58*, Space group *I-43 m*) and $Mg_{41}Sm_5$ (Pearson symbol *tI92*, Space group *I4/m*) compounds are in equilibrium with Mg-based solid solution in the associated binary systems.[13]

E.A. Lukyanova, A.A. Baikov Institute of Metallurgy and Materials Science, Russian Academy of Sciences, Leninsky Prospect 49, 119334 Moscow, Russia; and Laboratory of Hybrid Nanostructured Materials, National University of Science and Technology "MISIS", Leninsky Prospect 4, 119049 Moscow, Russia; **L.L. Rokhlin, T.V. Dobatkina, I.G. Korolkova,** and **I.E. Tarytina**, A.A. Baikov Institute of Metallurgy and Materials Science, Russian Academy of Sciences, Leninsky Prospect 49, 119334 Moscow, Russia. Contact e-mails: helenelukyanova@gmail.com, rokhlin@imet.ac.ru, and dobat@imet.ac.ru.

2. Experimental Procedures

2.1 Preparation of the Alloys

Alloys for the investigation were prepared using magnesium (99.96 mass%), dysprosium (99.83 mass%), and samarium (99.83 mass%). %) The alloys were melted in the electrical resistance furnace using low-carbon steel crucibles and a flux preventing the ignition of magnesium melts in air. Dysprosium and samarium made part of melt in the form of Mg-43 mass% Dy and Mg-30 mass% Sm master alloys prepared from the same starting metals. The flux containing 38-46% $MgCl_2$, 32-40% KCl, 3-5% CaF_2, 5-8%$BaCl_2$, 1,5% MgO, < 8% (NaCl + $CaCl_2$) (mass%) composition with the melting temperature of ~450 °C (determined by DTA) was used. Alloys were cast in a stainless steel chill mold. Ingots 15 mm in diameter and 90 mm in length and ~30 g in weigh were prepared. The ingots were cut into samples 15 mm in diameter, of 15 mm in length and of ~5 g in weigh, which were annealed successively at 500, 400 and 300 °C for 24, 50 and 100 h, respectively, in order to achieve the equilibrium state of the alloy structures. After each annealing the samples were quenched into room-temperature water to retain their structure. To ascertain that the annealing of alloys at 300 °C for 100 h is sufficient to bring them to the equilibrium state, samples were additionally annealed at this temperature for 100 h; in this case, the total time of annealing at 300 °C was 200 h. The electrical resistivity of samples annealed for 100 h and 200 h was measured. It is known that with increasing annealing time a magnesium solid solution is desaturated due to the precipitation of the second phase enrich in rare-earth metals. As the second phase precipitates the magnesium matrix becomes more conductive and the electrical resistivity of the alloy decreases. The annealing time at which the electrical resistivity ceases to drop and remains unchanged should be sufficient to achieve the equilibrium state, since no precipitation process occurs. Comparison of the alloys annealed at 300 °C for 100 and 200 h indicated the values of electrical resistivity to be almost identical for the alloys of similar compositions. Therefore, the annealings for 100 and 200 h could be considered equally sufficient to reach the equilibrium state at 300 °C in structures.

2.2 Investigation Techniques

The compositions of melted alloys were taken in accordance with the chemical analysis, which was performed by atomic emission spectroscopy using an ULTIMA 2C inductively coupled plasma spectrometer (Jobin-Yvon). To cover the entire area where the boundary of a magnesium solid solution may pass and the invariant transformation may take place, the alloys in an amount of ~40 of different composition were prepared. Compositions of the studied alloys are shown in the Gibbs triangle in Fig. 1.

As one can see, along with the ternary alloys containing Dy and Sm, the binary Mg-Dy and Mg-Sm alloys were also prepared for comparison. The annealed samples were used for metallographic studies and x-ray diffraction analysis.

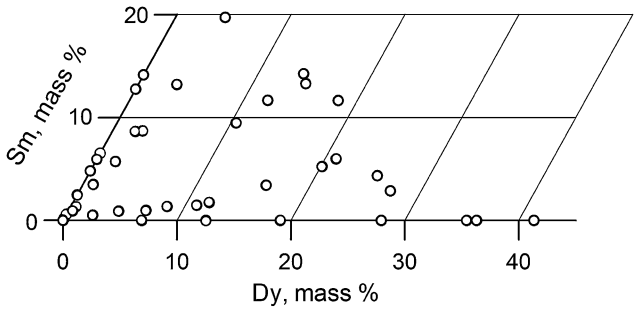

Fig. 1 Composition of the studied alloys

The microstructure was observed using optical and the scanning electron microscopy (SEM). For the optical microscopy, samples were subjected to mechanical grinding on successively finer abrasive papers, polishing and etching in 0.5 vol.% HNO_3 or 30 vol.% H_3PO_4 ethyl alcoholic solutions. Observations of the structures were conducted with a Reichert MeF (Austria) optical microscope. Scanning electron microscopy was performed on a LEO-430i scanning electron microscope equipped with a LINK-ISIS-300 energy-dispersive x-ray analyzer.

Qualitative x-ray diffraction analysis was performed using a Rigaku Ultima IV diffractometer, CuK_α radiation, and a θ angle range of 4-94°). Phases were identified using PDF2 Complete Database of International Committee of Crystallographic Data (ICCD), 2008.

Phase transformations in the alloys with a liquid phase were studied by differential thermal analysis (DTA). DTA curves were measured during cooling using a two-coordinate plane-table potentiometer H307 on samples of 6 g in weight. DTA was performed at heating and cooling rates of about 3 °C/min prevent the oxidation and burning of samples at high temperatures, they were covered with a flux containing 75%LiCl + 25%LiF (mass%).

3. Results and Discussion

3.1 Microstructure Observations

The typical microstructures of the alloys are presented in Fig. 2, which indicate the existence of only two second phases being in equilibrium with Mg-based solid solution. The compounds are $Mg_{24}Dy_5$ and $Mg_{41}Sm_5$, which also are in equilibrium with the Mg solid solution in the Mg-Dy and Mg-Sm binary system, respectively. Such a conclusion could be inferred based on the fact that the second phase observed in alloys of one of the binary systems, for example, Mg-Dy, retained its appearance in adding Sm up to the formation of the second phase typical of the other binary Mg-Sm system and vice versa. Some phases observed after annealing at 500 °C for 24 h are shown in Fig. 2(a) and (b). Each of the phases, according to the binary Mg-Dy and Mg-Sm phase diagrams, was formed as a part of the eutectic, which is finer for the Mg-Dy system. The $Mg_{24}Dy_5$ and $Mg_{41}Sm_5$ phases could be simultaneously observed in equilibrium with the Mg-based solid solution, excluding the

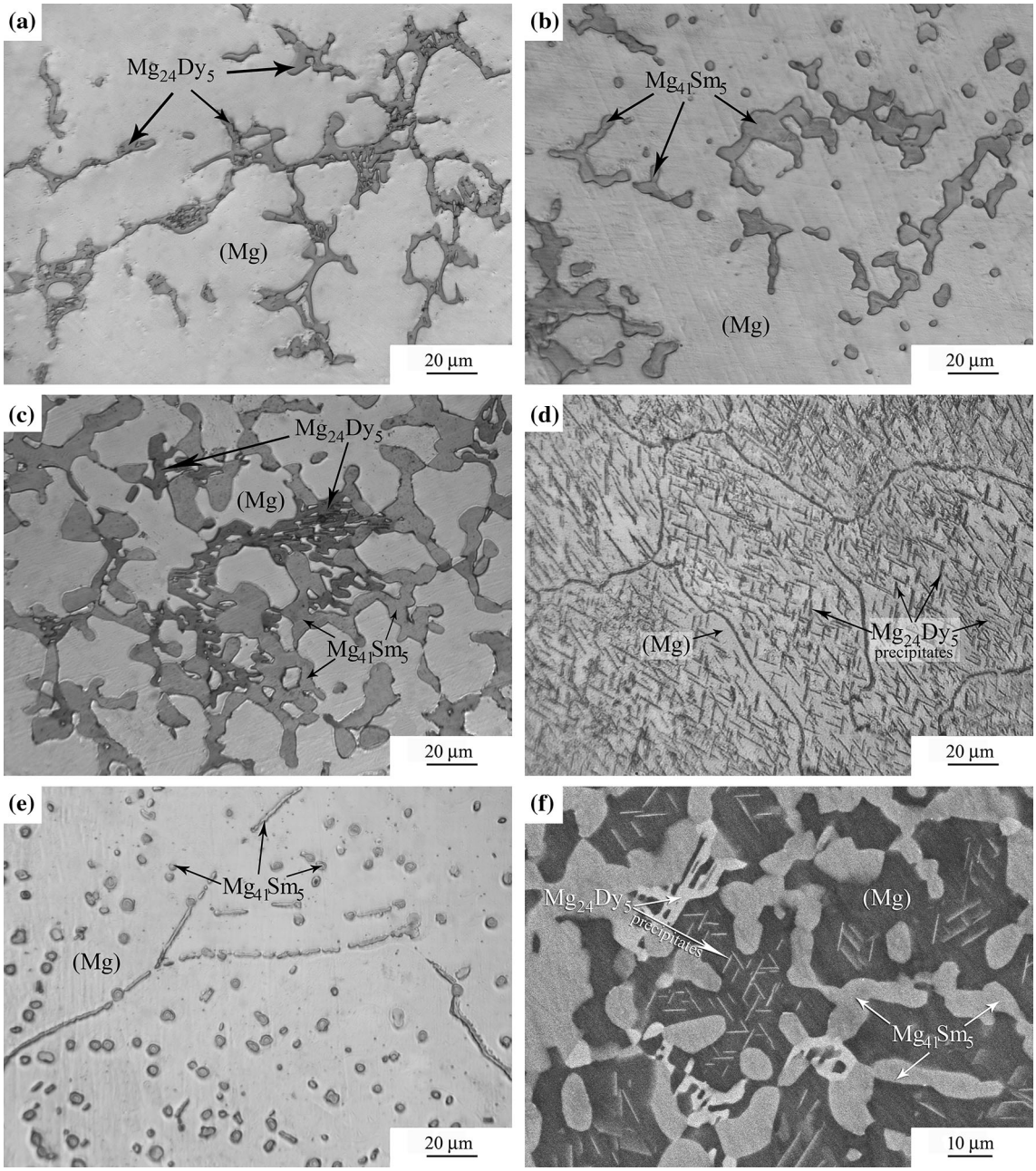

Fig. 2 Microstructures of the alloys (mass%) annealed at (a-c) 500 °C for 24 h, (d) 300 °C for 100 h and (e, f) 400 °C for 50 h: (a) Mg-21.0%Dy-6.0%Sm, (b) Mg-2.6%Dy-8.7%Sm, (c) Mg-14.0%Dy-14.2%Sm, (d) Mg-16.1%Dy-3.4%Sm, (e) Mg-2.5%Sm, and (f) Mg-14.0%Dy-14.2%Sm; (a-e) optical microscopy and (f) SEM micrographs

existence of any other second phase in equilibrium with the Mg solid solution. Such a microstructure observed in the optical microscope is shown in Fig. 2(c). In this case, the $Mg_{24}Dy_5$ phase containing the heavy rare-earth metal is darker.

After annealing at 500 °C, for 24 h, the microstructures of the alloys consist of sufficiently coarse second-phase crystals located among wide Mg-base solid solution fields. After subsequent annealing at 400 °C for 50 h and, after then, at 300 °C for 100 h, the Mg solid solution was decomposed. In these cases, fine particles enriched in the rare-earth metals precipitate from the Mg solid solution and could be observed. After annealing at 400 °C for 50 h, precipitated particles were coarser as compared to those precipitated after annealing at 300 °C for 100 h. Precipitates of the $Mg_{24}Dy_5$ or $Mg_{41}Sm_5$ phases differ in shape. The $Mg_{24}Dy_5$ precipitates are plate-like and located along certain atomic planes of the Mg lattice along three directions in grains (Fig. 2d). The $Mg_{41}Sm_5$ precipitates are rounded (Fig. 2e). Such a difference in the shapes of $Mg_{24}Dy_5$ and

$Mg_{41}Sm_5$ precipitates allows one to distinguish the phases in structure.

For a number of the alloys, both optical microscopy and SEM were used, and the consistent results on the existence of the phases in them were obtained. Figure 2(f) shows one of the SEM micrographs. Two second phases exist in structure of the alloy, but unlike the optical microscopy data, the $Mg_{24}Dy_5$ phase is seen to be brighter than $Mg_{41}Sm_5$. The microstructure of alloy annealed at 400 °C for 50 h is given in Fig. 2(f). Plate-like $Mg_{24}Dy_5$ precipitates in the Mg solid solution are observed. One of the Mg solid solution grains in the center of the micrograph indicates plate-like precipitates arranged with the three-fold symmetry.

3.2 Electron Probe Microanalysis

The electron probe microanalysis (EPMA) performed during SEM confirmed the existence of only two second $Mg_{24}Dy_5$ and $Mg_{41}Sm_5$ phases in the structure of the Mg-Dy-Sm alloys. The compositions of the second phases (see Table 1) were determined for two alloys and averaged for no less than 5 measurements (5 points). The main results show some deviations of the real second-phase compositions, in particular for $Mg_{24}Dy_5$, from the stoichiometric compositions corresponding to binary systems. In the case of ternary alloys, the higher magnesium content is observed. According to the stoichiometric composition, the $Mg_{24}Dy_5$ compound contains 41.8%Mg + 58.2%Dy (mass%) and the $Mg_{41}Sm_5$ compound contains 57.0%Mg + 43.0%Sm (mass%); the measured values are 51.6%Mg + 48.4%Dy (mass%) for $Mg_{24}Dy_5$ and 58.9%Mg + 41.1%Sm (mass%) for $Mg_{41}Sm_5$. However, the deviation of the compositions of real compounds from the stoichiometric compositions is sufficiently common phenomenon. It was observed also for the similar $Mg_{24}Y_5$ compound in the Mg-Y system, for which also the higher Mg content was observed.[17] The compound compositions in the binary and ternary systems point to the significant solubility of Sm in $Mg_{24}Dy_5$ and Dy in $Mg_{41}Sm_5$, which allows us to consider the compounds as the ($Mg_{24}Dy_5$) and ($Mg_{41}Sm_5$) solid solutions. Another remarkable feature consists in the closeness of Mg contents in these compounds in the binary and ternary systems. This fact allows us to conclude that the Sm dissolution in $Mg_{24}Dy_5$ actually is accompanied by the substitution of Sm for Dy atoms in the crystal lattice. The Dy dissolution in $Mg_{41}Sm_5$ actually is accompanied by the substitution of Dy for Sm atoms in the crystal lattice. Any changes of the compound compositions of the both phases, which were observed with changing annealing temperature and any signs of their decomposition, which are observed with decreasing annealing temperature, were not reliably established.

The EPMA was used also to study the Mg-based solid solution in the cases of its equilibrium with one or two second phases. The comparison of EPMA data with those available in the literature for the binary systems Mg-Dy, Mg-Sm[14,16] agree adequately. For example, the EPMA of the binary two-phase Mg-Dy and Mg-Sm alloys annealed at 500 °C for 24 h showed that the Dy and Sm solubility in solid Mg is 23.1 mass% Dy (4.3 at.% Dy) and 4.0 mass% Sm (0.7 at.% Sm), respectively; according literature data, the solubilities are 22.5 mass% Dy (4.2 at% Dy)[14] and 4.3 mass% Sm (0.7 at.% Sm).[16] The EMA was used to determine the Mg solid solution composition in the alloys containing the $Mg_{24}Dy_5$ and $Mg_{41}Sm_5$ phases simultaneously (three-phase equilibrium). The data obtained for the studied annealing temperatures are presented in Table 2.

3.3 X-Ray Diffraction Analysis

X-ray diffraction analysis was used only to identify solid phases, which are in equilibrium with Mg-based solid solution in the alloys. X-ray diffraction patterns of the $Mg_{24}Dy_5$ and $Mg_{41}Sm_5$ phases are characterized by numerous weak reflections that make them difficult to be identified in the experimental patterns of the alloys. Nevertheless, the x-ray diffraction analysis has confirmed results of metallographic analysis data, namely, the fact that only the $Mg_{24}Dy_5$ and $Mg_{41}Sm_5$ are in equilibrium with the Mg solid solution. Figure 3 the x-ray diffraction pattern the alloy, which was annealed at 500 °C for 24 h (to bring it to equilibrium state) and contains two second phases and Mg solid solution It is seen the reliable coincidence of the main diffraction reflections of Mg (blue) and $Mg_{41}Sm_5$ (red) in bar diagrams available in PDF2 Complete Database of ICCD with the reflections in the experimental x-ray diffraction pattern. This confirms the existence of the $Mg_{41}Sm_5$ phase in the studied alloy. The coincidence of the $Mg_{24}Dy_5$ diffraction reflections in the bar diagram (green) with the reflections in the experimental x-ray diffraction pattern also confirms the existence of this phase; however, its presence is not so clear. Since the Dy solubility in solid Mg is higher than that of Sm, the content of the $Mg_{24}Dy_5$ phase is lower than that of $Mg_{41}Sm_5$.Taking into account the lower content of the $Mg_{24}Dy_5$ phase, its x-ray reflections are not so intense. Therefore, in this study, the

Table 1 The compositions of the $Mg_{24}Dy_5$ and $Mg_{41}Sm_5$ phases in the binary Mg-Dy, Mg-Sm and ternary (three-phase equilibrium) (EPMA data)

System	Phase	Composition, mass%			Composition, at.%		
		Mg	Dy	Sm	Mg	Dy	Sm
Mg-Dy	$Mg_{24}Dy_5$	51.6	48.4	0	87.7	12.3	0
Mg-Sm	$Mg_{41}Sm_5$	58.9	0	41.1	89.9	0	10.1
Mg-Dy-Sm	$Mg_{24}Dy_5$	51.0	23.6	25.4	87.0	6.0	7.0
Mg-Dy-Sm	$Mg_{41}Sm_5$	56.9	9.2	33.9	89.2	2.2	8.6

Table 2 The composition of the Mg solid solution being in the three-phase equilibrium with the $Mg_{24}Dy_5$ and $Mg_{41}Sm_5$ phases at different temperatures (EPMA data)

	Composition, mass%			Composition, at.%		
Temperature, °C	Mg	Dy	Sm	Mg	Dy	Sm
500	81.5	13.4	5.1	96.7	2.3	1.0
400	87.4	10.1	2.5	97.8	1.7	0.5
300	91.1	7.5	1.4	98.5	1.3	0.2

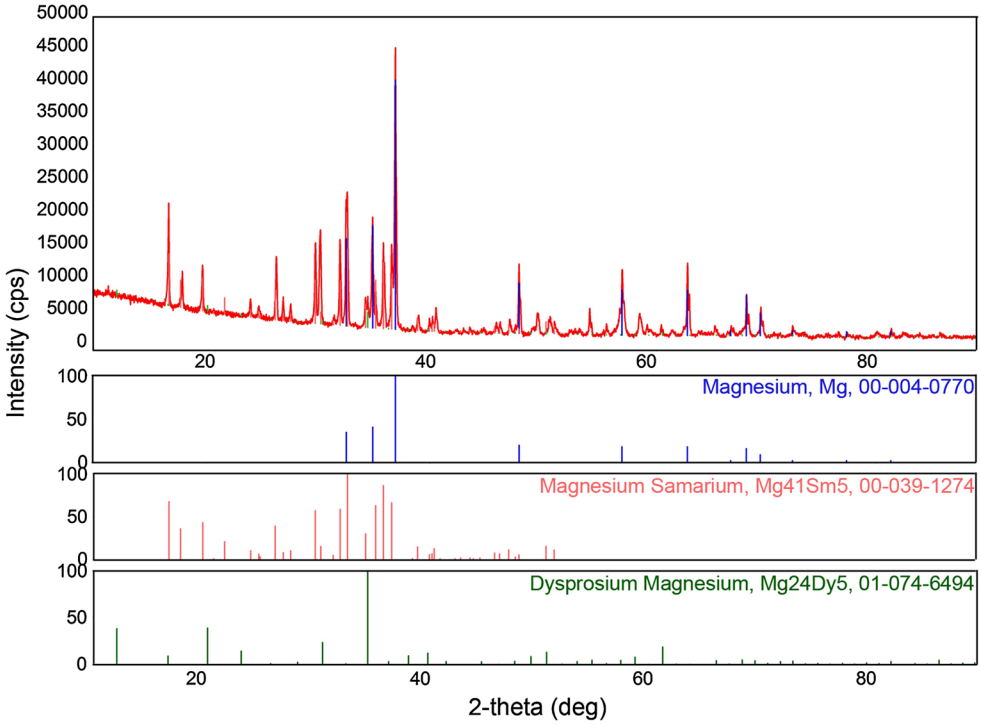

Fig. 3 Experimental x-ray diffraction pattern for the Mg-14.0% Dy-14.2% Sm (mass%) alloy annealed at 500 °C for 24 h (top picture) and bar diagrams for Mg, Mg41Sm5 and Mg24Dy5 available in the PDF2 Database (ICCD)

EPMA data are considered to be more reliable as compared to x-ray diffraction data.

3.4 Isothermal Sections

Microstructure observations, x-ray diffraction analysis and EPMA allowed us to construct the partial isothermal sections of the Mg-Dy-Sm phase diagram at 500, 400 and 300 °C for the Mg-rich alloys (Fig. 4, 5, 6). Symbols in the sections correspond to EMA data for the Mg solid solution and compounds. The isothermal sections demonstrate the substantial narrowing the Mg solid solution regions with decreasing temperature.

3.5 Differential Thermal Analysis

Two critical temperatures can be determined by DTA; these are the temperature of the onset of the liquid solidification (liquidus temperature) and the temperature of the start of the three-phase reaction or temperature of the four-phase invariant equilibrium with the participation of

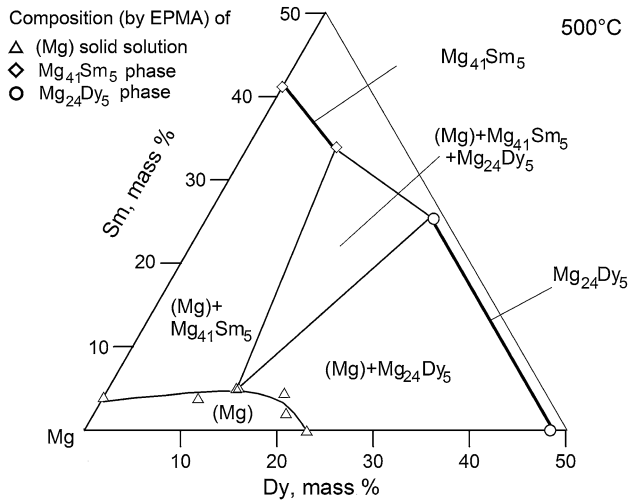

Fig. 4 Partial isothermal section of the Mg-Dy-Sm phase diagram for Mg-rich alloys at 500 °C

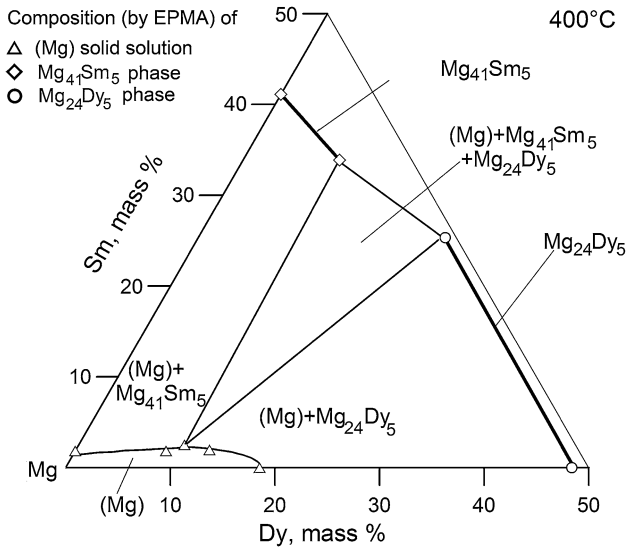

Fig. 5 Partial isothermal section of the Mg-Dy-Sm phase diagram for Mg-rich alloys at 400 °C

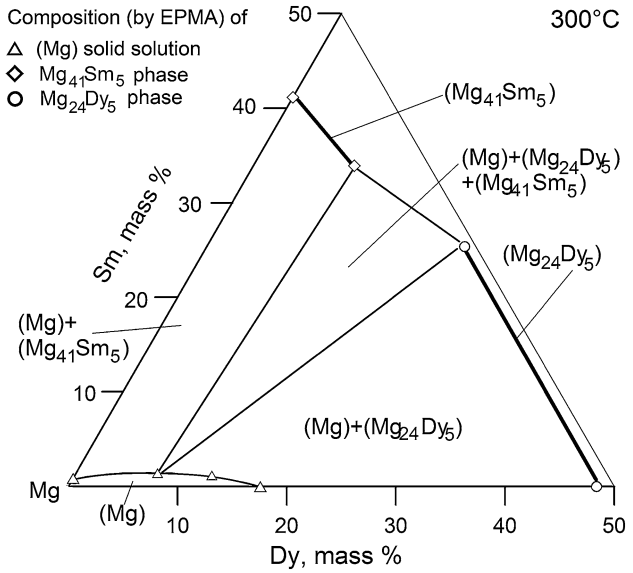

Fig. 6 Partial isothermal section of the Mg-Dy-Sm phase diagram for Mg-rich alloys at 300 °C

liquid phase. The latter could be supposed taking into consideration the two solid second phases being in equilibrium with Mg solid solution in the solid state. All the above transformations that during cooling give sufficiently high thermal effects. The analysis of the DTA data indicates that temperature of the invariant four-phase equilibrium between (Mg), ($Mg_{24}Dy_5$), ($Mg_{41}Sm_5$) and liquid phase (L) is 535 °C. This value was found to be higher than the determined temperature of eutectic transformation, 526 °C, in the binary Mg-Sm system and lower than the temperature of eutectic transformation, 563 °C, in the binary Mg-Dy system. Therefore, we conclude that the invariant four-phase

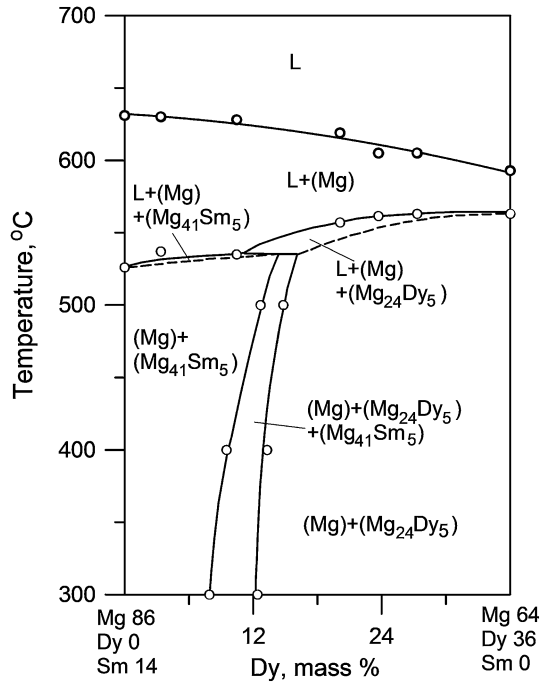

Fig. 7 Temperature-composition section of the Mg-Dy-Sm phase diagram from Mg-36mass% Dy to Mg-14mass% Sm

equilibrium is of the transition type, L + ($Mg_{24}Dy_5$) ⇆ (Mg) + ($Mg_{41}Sm_5$).

3.6 Temperature-Composition Section

The DTA data were used to construct the temperature-composition section opposite the Mg corner of the phase diagram, which connects the Mg-36mass%Dy and Mg-14mass%Sm compositions. The section is shown in Fig. 7. It indicates the phase regions adjoining to the Mg solid solution and their mutual arrangement.

3.7 The Overall View of the Mg-Rich Part of the Mg-Dy-Sm Phase Diagram

Taking into account the constructed sections and the established invariant reaction, the overall view of the Mg-rich part of the Mg-Dy-Sm phase diagram was constructed, which gives more detailed information about the diagram as a whole (Fig. 8). The overall view indicates the region, within which a transformation occurs, provides insight into the nature of phase transformations, their temperature ranges and sequence. In the overall view, the four-phase invariant equilibrium plane is shown by the ABCD quadrangle. Compositions of the phases, which take part in the invariant equilibrium, are given in Table 3.

The compositions of the ($Mg_{24}Dy_5$) and ($Mg_{41}Sm_5$) solid solutions are assumed to be unchanged at 300, 400 and 500 °C (Table 1). The composition of magnesium solid solution (Mg) was estimated by extrapolation of the Dy and Sm contents in it at 300, 400 and 500 °C to an invariant equilibrium temperature of 535 °C. When extrapolating, the composition of the liquid phase participating in the invariant

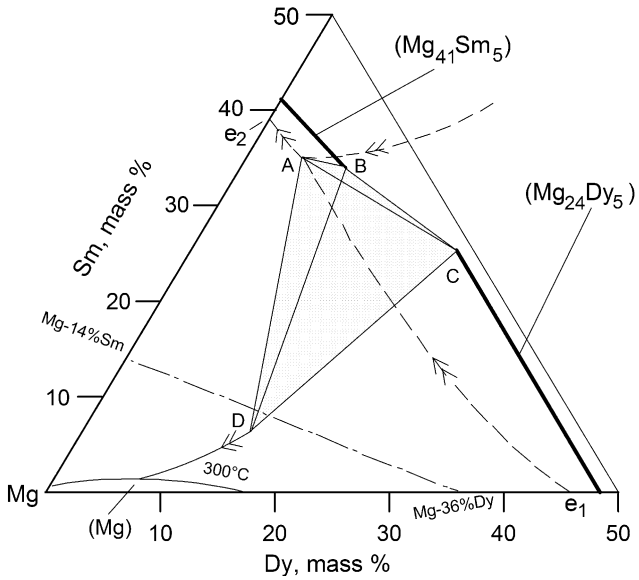

Fig. 8 The overall view of the Mg-rich part of the Mg-Dy-Sm phase diagram

Table 3 Composition of the phases participating in the invariant four-phase equilibrium L + ($Mg_{24}Dy_5$) ⇆ (Mg) + ($Mg_{41}Sm_5$) in the Mg-rich alloys of the Mg-Dy-Sm system

	Element Content, mass%		
Phase	**Mg**	**Dy**	**Sm**
L	~60	~5	~35
($Mg_{24}Dy_5$)	51.0	23.6	25.4
(Mg)	78.9	14.8	6.3
($Mg_{41}Sm_5$)	56.9	9.2	33.9

equilibrium was established approximately assuming that it corresponds to the point of intersection of the double saturation (Mg) + ($Mg_{41}Sm_5$) line and a straight line running from the point of (Mg) at the invariant equilibrium plane and passes the edge of the line of invariant equilibrium plane in the temperature-composition section (Fig. 7). At the same time, the double saturation (Mg) + ($Mg_{41}Sm_5$) line was assumed to run to the binary Mg-Sm eutectic point almost in parallel to the constant Mg-contents lines in the concentration triangle, since, according to metallographic analysis data, Dy added to the Mg-Sm alloys does not change the view of the Mg + $Mg_{41}Sm_5$ eutectic. The three-phase equilibria with the participation of liquid (Fig. 8) are shown tentatively by the dashed lines. The Mg-Dy and Mg-Sm eutectic points are designated by $e_1$and e_2, respectively. In Fig. 8, the temperature-composition section-line from Mg-36mass% Dy to Mg-14mass% Sm also is indicated.

This investigation indicated that peculiarities of the constructed Mg-rich portion of the Mg-Dy-Sm phase diagram are similar to those observed in the analogous portions of the phase diagrams of other studied Mg-containing ternary systems with two rare-earth metals from different, yttrium and cerium groups, namely, Mg-Y-Nd,[18] Mg-Y-Sm,[19] and Mg-Y-La.[20] These features are the (1) absence of any other solid phase in equilibrium with Mg solid solution, (2) except the riches by Mg compounds in equilibrium with Mg solid solution in the respective binary systems and (3) certain solubility of each of rare-earth metals in the Mg compounds with the other rare-earth metal. The difference between the various ternary phase diagrams of this type consists in the extension of the respective phase regions, in particular, in the extension of the Mg-based solid solution, temperatures of the invariant equilibria, and the solubility of one of the rare-earth metals in the Mg-rich compound with the other rare-earth metal. In this work, the above mentioned regularities were confirmed for the Mg-Dy-Sm phase diagram and the specific values of the main parameters of it were determined.

4. Conclusions

The Mg-rich part of the ternary Mg-Dy-Sm phase diagram was studied experimentally for the first time. The following can be concluded:

1. Only two solid phases, $Mg_{24}Dy_5$ and $Mg_{41}Sm_5$, are in equilibrium with the Mg-based solid solution in the Mg-Dy-Sm system; each of the compounds are the Mg-rich compound in the binary Mg-Dy and Mg-Sm systems.
2. The significant both Sm solubility in $Mg_{24}Dy_5$ and Dy solubility of Dy in $Mg_{41}Sm_5$ were found; the rare-earth elements substitutes each other with actually substitution of Sm.
3. The existence of the four-phase invariant equilibrium of transition type L + ($Mg_{24}Dy_5$) ⇆ (Mg) + ($Mg_{41}Sm_5$) at 535 °C was established in the Mg-Dy-Sm system, in which (Mg), ($Mg_{24}Dy_5$) and ($Mg_{41}Sm_5$) are the solid solutions based on magnesium and corresponding compounds. Compositions of the phases participating in this invariant equilibrium were determined.
4. Three partial isothermal sections at 500, 400, 300 °C and one temperature-composition section from Mg-36-mass% Dy to Mg-14mass% Sm were constructed. The sections indicate the existing phase regions, including the extended Mg solid-solution region, their arrangement and sizes in the Mg-rich portion of the Mg-Dy-Sm phase diagram.

Acknowledgment

The work was supported by the Russian Foundation for Basic Research (Project No. 15-03-01351-A). The authors gratefully appreciate the financial support of the Ministry of Education and Science of the Russian Federation provided

in the framework of the Program aimed to increase the competitiveness of the National University of Science and Technology "MISIS".

References

1. B.L. Mordike and T. Ebert, Magnesium: Properties-Applications-Potential, *Mater. Sci. Eng., A*, 2001, **302**, p 37-45
2. E. Aghion and D.Elizer, Eds., *Magnesium Alloys. Science, Technology and Applications* ,Published by the Israeli Consortium for the Development of Magnesium Technology. S.Neaman Institute, Technion City, Haifa 3200, 2004
3. S. Zhu, M.A. Easton, T.B. Abbott, J.F. Nie, M.S. Dargusch, N. Hort, and M.A. Gidson, Evaluation of Magnesium Die-Casting Alloys for Elevated Temperature Applications: Microstructure, Tensile Properties and Creep Resistance, *Metall. Mater. Trans. A*, 2015, **46A**, p 3543-3554
4. A. Luo and M.O. Pekguleryuz, Cast Magnesium Alloys for Elevated Temperature Applications, *J. Mater. Sci.*, 1994, **29**, p 5259-5271
5. C.J. Bettles and M.A. Gibson, Curent Wrought Magnesium Alloys: Strength and Weakness. *JOM (Previously Journal of Metals),* 2005, p 46-49
6. Z. Yang, J.P. Li, J.X. Zhang, G.W. Lorimer, and J. Robson, Review on Research and Development of Magnesium Alloys, *Acta Metall. Sin. (Engl. Lett.),* 2008, **21**(5), p 313-328
7. L.L. Rokhlin, *Magnesium Alloys Containing Rare Earth Metals*, Taylor & Francis, 2003
8. X.B. Liu, R.S. Chen, and E.H. Han, Effects of Ageing Treatment on Microstructures and Properties of Mg-Gd-Y-Zr Alloys with and Without Zn Addition, *J. Alloy. Compd.*, 2008, **465**, p 232-238
9. P.J. Apps, H. Krimzadeh, J.F. King, and G.W. Lorimer, Precipitastion Reactions in Magnesium-Rare Earth Alloys Containing Yttrium, Gadolinium or Dysprosium, *Scr. Mater.*, 2003, **48**, p 1023-1028
10. L. Zhang, J. Zhang, Z. Leng, S. Liu, Q. Yang, R. Wu, and M. Zhang, Microstructure and Mechanical Properties of High Performance Mg-Y-Er-Zn Alloys, *Mater. Des.*, 2014, **54**, p 256-263
11. V. Neubert, I. Stulikova, B. Smola, B.L. Mordike, M. Vlach, A. Bakkar, and J. Pelkova, Thermal Stability and Corrosion Behavior of Mg-Y-Nd and Mg-Tb-Nd Alloys, *Mater. Sci. Eng., A*, 2007, **A462**, p 329-333
12. L. Yang, Y. Huang, F. Feyerabend, R. Willumeit, C. Mendis, K.U. Kainer, and N. Hort, Microstructure, Mechanical and Corrosion Properties of Mg-Dy-Gd-Zr Alloys for Medical Applications, *Acta Biomater.*, 2013, **9**, p 8499-8508
13. Binary Phase Diagrams, 2nd ed., T.B. Massalski (Editor-in-chief), ASM International, Materials Park, OH, 1990
14. L.L. Rokhlin and L.P. Deeva, Magnesium Alloys with Dysprosium, *Technolog. Legkich Splavov*, 1976, No. 12, p 83-84 (**in Russian**)
15. A. Saccone, S. Delfino, G. Brozone, and R. Ferro, The Samarium-Magnesium System: A Phase Diagram, *J. Less-Common Met.*, 1989, **154**(1), p 47-60
16. L.L. Rokhlin, E.M. Padezhnova, and L.S.Guzey, Investigation of the Samarium Solubility in the Mg-Base Solid Solution. *Izv. AN SSSR, Metally*, 1976, No. 6, p 204-208 (**in Russian**)
17. J.F. Smith, D.M. Bailey, D.B. Novotny, and J.E. Davison, Thermodynamics of Formation of Yttrium-Magnesium Intermediate Phases, *Acta Metall.*, 1965, **13**(8), p 889-895
18. Z.A. Sviderskaya and E.M. Padezhnova, Solubility of Neodimium and Yttriumin in Solid Magnesium. *Izv. AN SSSR, Metally*, 1971, No. 6, p. 200-204 (**in Russian**)
19. R. Schmid-Fetzer, N. Bochvar, and R. Stroug, *Magnesium-Samarium-Yttrium. Ternary Alloys. A CmprehensiveCompedium of Evaluated Constitutional Data and Phase Diagrams. V.18*, G. Effenberg, F. Aldinger, and P. Rogl., Eds., Published by MSI, Stuttgart (Federal Republic of Germany), 2001, p 629-641
20. E.M. Padezhnova, T.V. Dobatkina, and E.V. Muratova, About the Mg-Y-La Phase Diagram in the Mg-Rich Area. *Izv. AN SSSR, Metally*, 1983, No. 4, p 194-197, in Russian